Microscopic origin of near- and far-field contributions to tip-enhanced optical spectra of few-layer MoS_2

Supplementary Information

Kathrin Kroth, Philip Klement, Limei Chen, Sangam Chatterjee, and Peter J. Klar *

Temperature and laser-power dependent measurements

The results of the temperature and laser-power dependent Raman and photoluminesence measurements are shown in Fig. S1 and S2, respectively. Essentially the same experimental setup was used as for the TERS/TEPL measurements, only without employing the MV2000 inset of Nanonics. A 1800 lines/mm diffraction grating was mounted inside the spectrometer for both measurements. For the temperature dependent measurement, a custom-made sample stage with an integrated Peltier element was used to control the substrate temperature in a range of 10 °C to 95 °C. The power of the laser (532 nm) was set to 2.48 mW at the sample surface in those measurements.

Impact of the TERS tips and the Si/SiO_2 substrate

As is well known, the enhancement is significantly influenced by the choice of the TERS tip and the underlying substrate. Here, we show that the enhancement also depends on the substrate morphology. Fig. S3 a) shows three different MoS_2 flakes consisting of few-layer (1-3L) and multilayer areas (MuL). While few-layers were confirmed by Raman spectroscopy, the layer thickness of the multilayer regions could only be classified by optical contrast imaging in sections I-VI of the sample. As already evident from the optical contrast of the SiO_2 layer, the flakes were exfoliated from a natural bulk crystal onto two different Si/SiO_2 substrates. Flake 1 and 2 were transferred onto Si substrates with a 275 nm thick wet thermal oxide layer (Siegert Wafer GmbH, Aachen, Germany). The SiO_2 layer at Flake 3 is 300 nm thick and was grown in a thermal dry/wet/dry cycle, which produces a high-quality oxide layer at the interfaces (MicroChemicals GmbH, Ulm, Germany). In Fig. S4, AFM images of the different Si/SiO_2 substrates are shown and exhibit a somewhat different surface morphology. All glass fibre TERS-tips, which are functionalized with Au nanoparticles, were acquired commercially (Nanonics Imaging Ltd, Jerusalem, Israel). In order to quantify the enhancement of TERS, the two Raman modes were fitted by two Lorentzian profiles and the ratio of the areas of the tip-in and the tip-out spectrum were calculated. As already discussed in the main article for Flake 1, the effective enhancement was deliberately not calculated by multiplying an additional weighting factor, since not all differences in the tip-in spectra can solely be attributed to near-field effects. The layer dependent enhancement factors of the two Raman modes are given in Fig. S3b). While the enhancement of the 1L and the MuL area of Flake 2 are on the same order of magnitude as those of Flake 1, significantly higher enhancement factors can be observed for the few-layers and the thinner MuL areas of Flake 3 (see Fig. S3 c)). Furthermore, differences in the course of the layer-dependent enhancement can be recognized. Analogous to Flake 1, also a counterintuitive, stepwise increase of the enhancement factor can be observed for Flake 3, but the maximum is not achieved for the MuL. In total, five different TERS tips (Tip A-E) were used for the measurements, but it is unlikely that these enormous differences can be attributed solely to variations in the tips due to manufacturing. Furthermore, no significant aging effect of the tips could be observed during the measurements. The numerical labelling of the measurements does not reflect the chronological order of the measurements (and some of the data were recorded on different days). For example, the measurement sequence for Tip A is 3L-2L-1L-MuL, whereby the first und last measurement points show the highest enhancements at this flake. Instead even the substrate morphology seems to play a crucial role. Although we use SiO_2 substrates only, clear differences in the enhancement of the Raman signals is observed when using substrates of different sources, i.e., with the SiO_2 layer prepared by different recipes. The SiO_2 layers are of the same chemical composition and differ solely in their structural properties such as layer thickness by 10% and morphology. These structural differences are sufficient to alter the interaction between MoS_2 and the underlying substrate area.

PCA of two classes of Raman spectra

To better highlight the differences between the three classes, additional PCA was performed for the Raman Data of 1L and 2L MoS_2. In contrast to the analyses in the main article, these were performed for only two classes of spectra. This means that the tip-enhanced spectra were analyzed one time the temperature dependent spectra only and another time with the laser power dependent spectra only. Corresponding PCA results of the different pairs of classes of Raman spectra are displayed in Fig. S5 and S6, respectively. Whereby, the

I. Physikalisches Institut und Zentrum für Materialforschung (ZfM/LaMa), Justus-Liebig-Universität Giessen, Heinrich-Buff-Ring 16, 35392 Giessen, Germany.
E-mail: Peter.J.Klar@physik.uni-giessen.de

score plots are shown in the upper part and the corresponding PC loadings as well as the average spectrum are plotted in the lower of the part of the figure for each pair of classes. In the PCA the eigenvalues of the covariance matrix are the principal components and the corresponding eigenvectors are the PC loadings. The PC loadings point along the directions of the principal axes (PCs) of the new coordinate system. The PC scores are the transformed coordinates of each spectrum, which are now represented as a single point.

In the score plots, a clear separation between the two classes is obtained in all cases except for the set consisting of the temperature dependent and the tip-enhanced spectra of the 2L MoS_2 samples. At this point, it should be noted that the spectra of the class of the tip-in spectra fall into two subgroups, consisting of 2 and 3 spectra. The two groups of spectra (as well as the temperature dependent spectra) were recorded on 2L areas of different MoS_2 flakes. Thus it seems that these areas are somewhat different, e.g., in terms of strain or the interactions with surface impurities. However, both groups of tip-enhanced spectra are well separable from the class of temperature dependent spectra. This indicates that there must exist an additional microscopic process other than the heating and field-enhancement, at least.

In the following, a short discussion of loadings and scores will be given. This is carried out exemplary on a TERS spectrum and on a Raman spectrum, which were recorded with a laser power of 0.22 mW. The corresponding spectra in the score plots of Fig. S6 are highlighted from the other spectra by filled symbols.

The experimental spectra can be written as follows:

$$S(\nu) = \tilde{S} + \sum_{i=1}^{N} PCi \cdot Li(\nu) \tag{1}$$

whereby $\tilde{S}$ is the average spectrum, *PCi* and *Li* are the scores and the loadings to the i-th eigenvalues, respectively. Thus, the loading curves provide information about possible trends with respect to the average of all spectra included in the analysis. In our specific example, L1, which belongs to PC1, mainly causes an intensity change of the A_{1g} mode. On the other hand, L2 mainly leads to a shift of both Raman modes, whereby this shift can be compensated for the E_{2g} mode by L1. The exemplary TERS spectrum has a positive PC1 and a slightly negative PC2 value. Compared to the average spectrum, one can predict an red-shift and a decrease in intensity of the A_{1g} mode. For the laser power dependent spectrum, PC1 is negative and PC2 is positive. This results in a blue-shift of the A_{1g} mode and the negative PC1 value causes an increase in intensity for this mode. For both example spectra, the shift of the E_{2g} mode is compensated by the opposite signs of PC1 and PC2. That these predictions are correct can easily verified by Fig. S7. Here, the experimental and the average spectrum for both examples are shown in red and black, respectively. The dotted graph represents the recalculated spectra using Eq. 1, taking into account the first three PCs. As expected, the deviation between the calculated and the experimental spectra are small, since the first three components already carry 92.62% of the variance weight for this PCA.

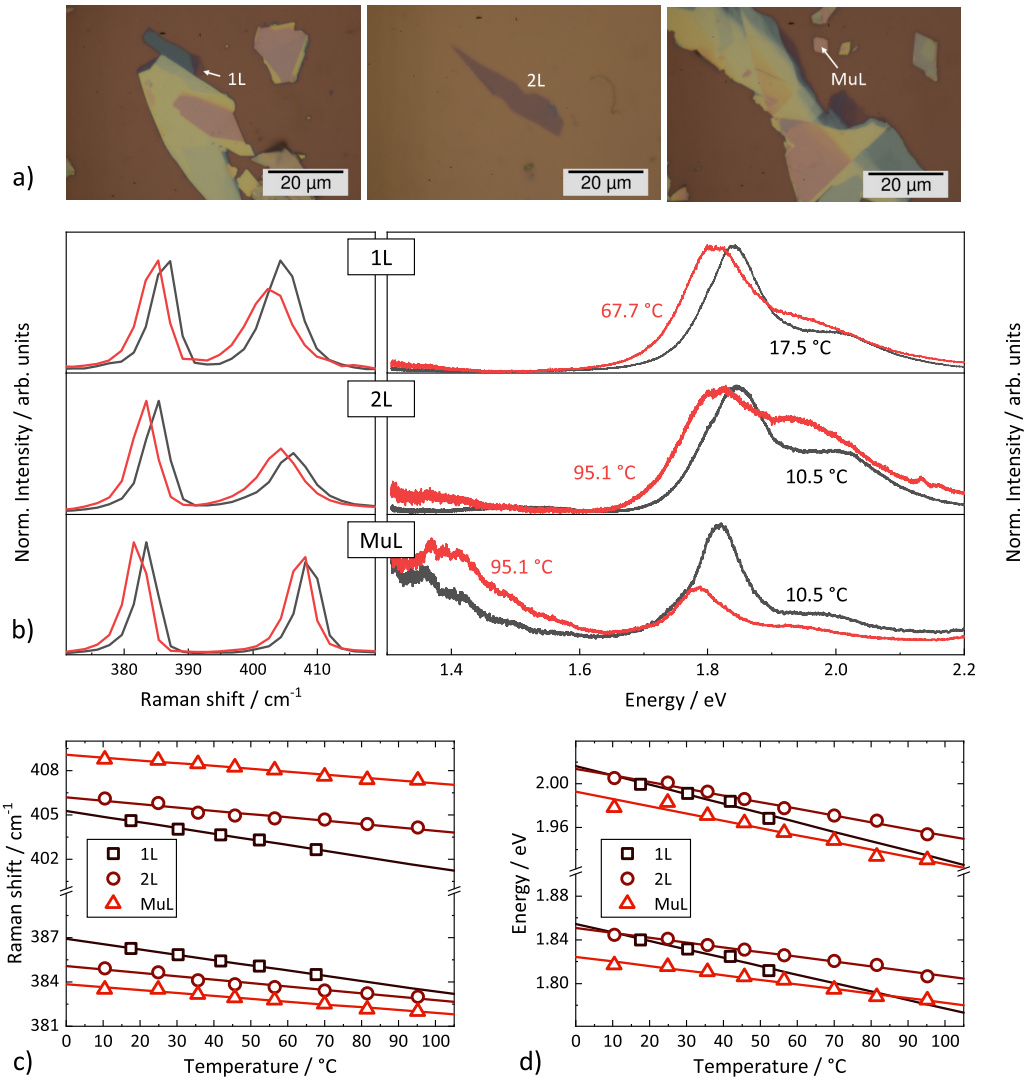

Fig. S1 Temperture-dependent measurements of MoS_2 sheets of different MoS_2 layer number on a Si/SiO_2 substrate. a) Optical microscope images of the investigated MoS_2 sheets. The areas of the in b) examined areas are marked with an arrow. b) Raman an PL spectra of different MoS_2 layers, exemplary recorded for two temperature settings. When the temperature increases, the Raman modes and the direct PL transitions exhibit a linear red-shift. c) Temperature dependence of the positions of the A_{1g} and E_{2g} Raman modes and d) the direct PL transitions A and B. For clarity, the Raman and PL spectra were normalized and the PL spectra of the multilayer MoS_2 sample were additionally smoothed.

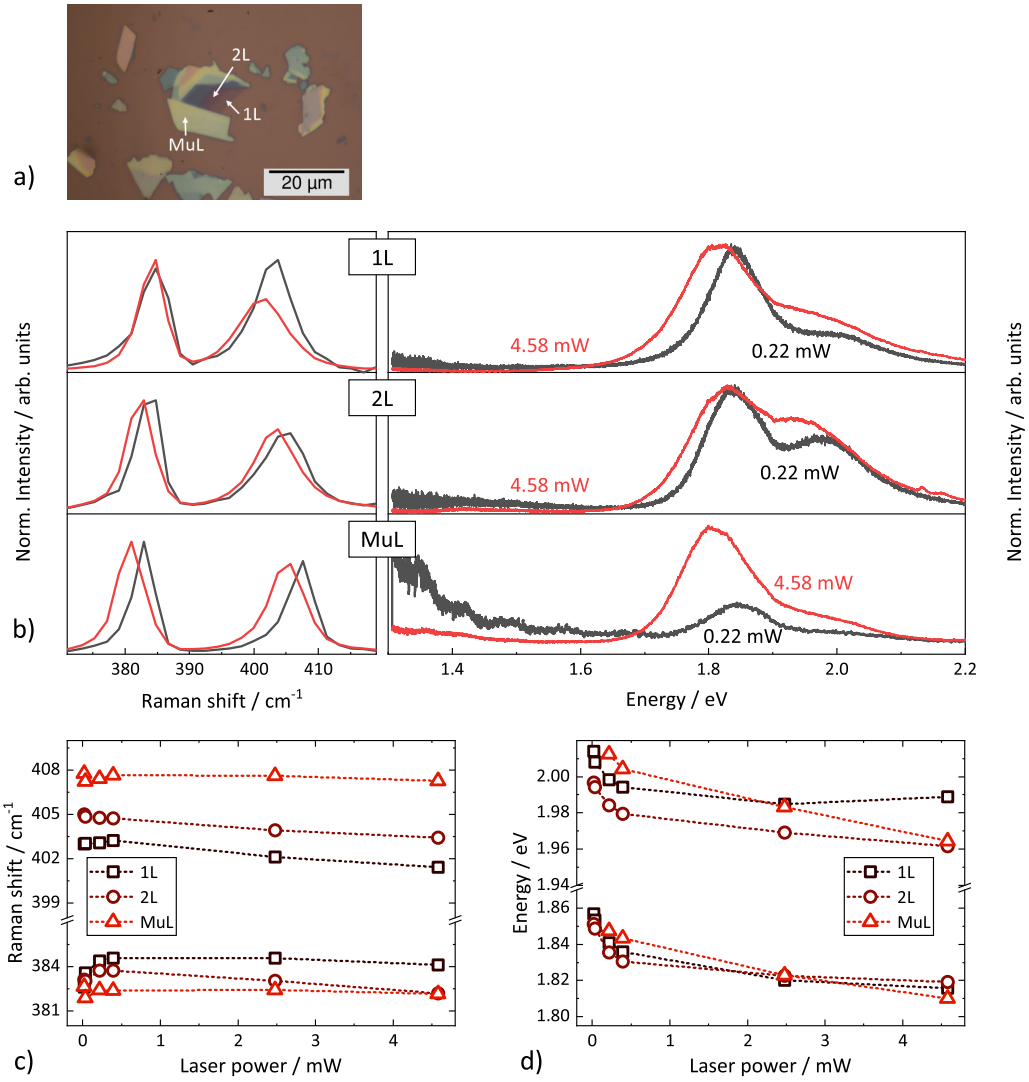

Fig. S2 Laser-power dependent measurements of different layered MoS_2 on Si/SiO_2 substrate. a) Optical microscope image of the investigated MoS_2 flake exhibiting areas of different layer number. The associated areas are marked with arrows. b) Raman and PL spectra of different MoS_2 layers, exemplarily recorded for two laser powers. c) Laser-power dependence of the positions of the A_{1g} and E_{2g} Raman mode and d) the direct PL transitions. For clarity, the Raman and PL spectra were normalized and the PL spectra of the multilayer sample were additionally smoothed.

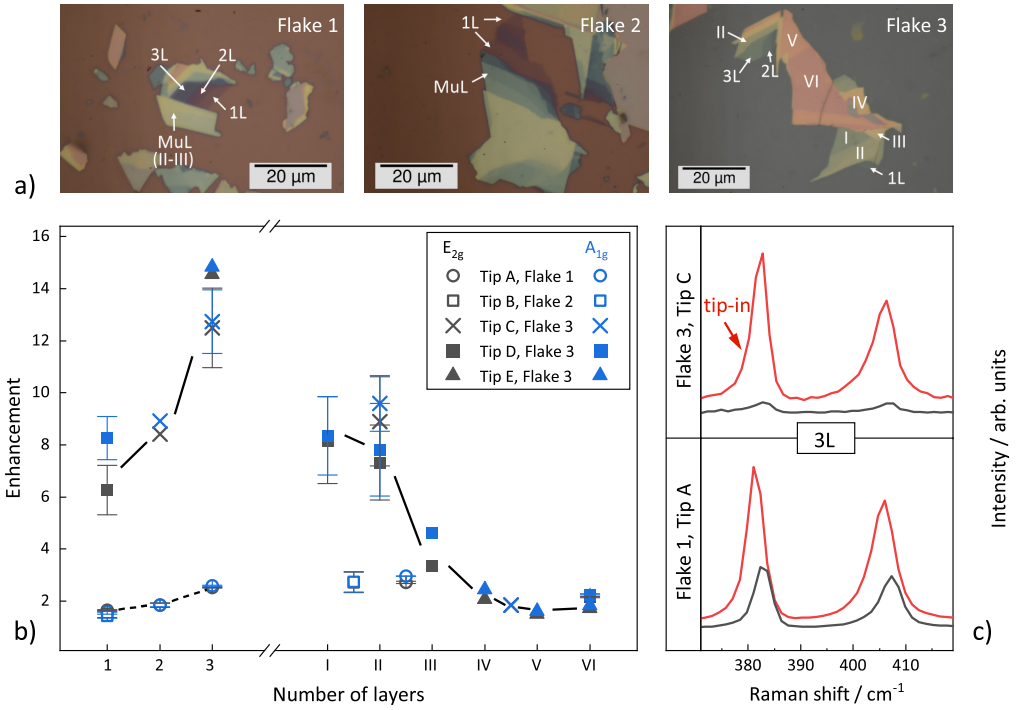

Fig. S3 Enhancement of TERS as a function of the layer thickness. a) Optical microscope images of three MoS_2 multi-stage flakes on two different types Si/SiO_2 substrates. While the 1-3L were confirmed by Raman spectroscopy, the layer thickness of the multilayer regions (I-VI) was classified by optical contrast imaging only. b)Enhancement of the Raman modes as a function of the layer thickness. Significant differences, in the profile as well as the magnitude of the enhancement, are apparent. c) Comparison of the TERS spectra of Flake 1 and 3 for 3L MoS_2, the sheets are exfoliated on different Si/SiO_2 substrates.

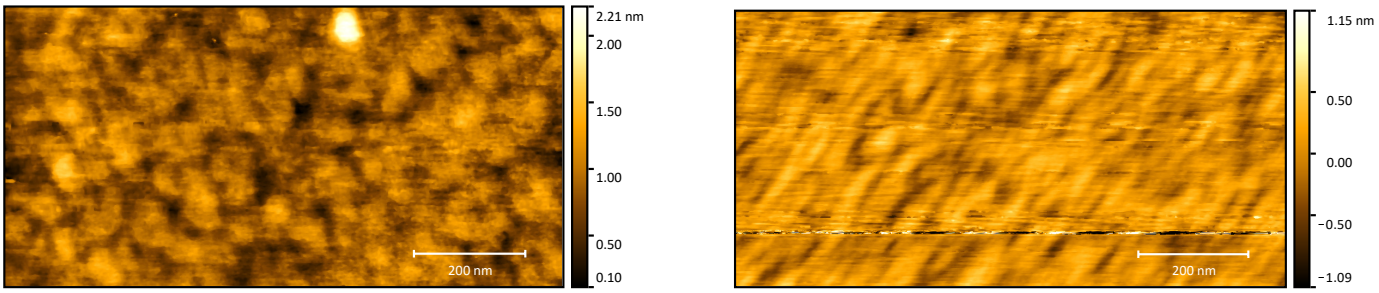

Fig. S4 AFM images of the two different Si/SiO_2 substrates. On the left the topography of the SiO_2 layer grown in a dry/wet/dry cycle (MicroChemicals GmbH, Ulm, Germany) and on the right the substrate with the wet thermal oxide layer (Siegert Wafer GmbH, Aachen, Germany).

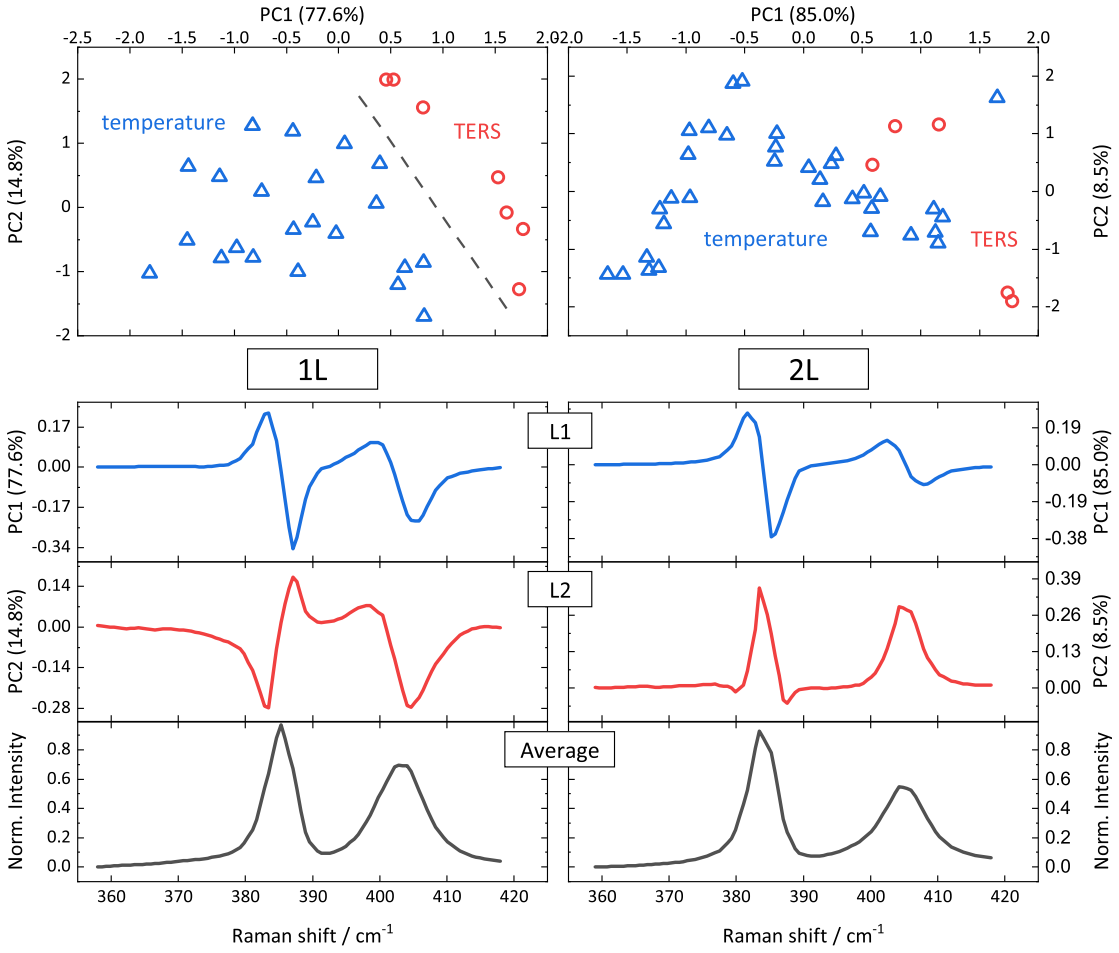

Fig. S5 PCA results of 1L and 2L MoS_2 tip-in and temperature dependent Raman spectra on the left and right, respectively. The upper part shows the PCA score plots. A clear separation of the two classes of spectra can be observed for 1L MoS_2. In case of the 2L MoS_2 spectra two groups of TERS spectra are formed which are separated from the temperature dependent data. The two groups correspond to two different samples. The corresponding PC loadings and the average spectra are given in the lower part.

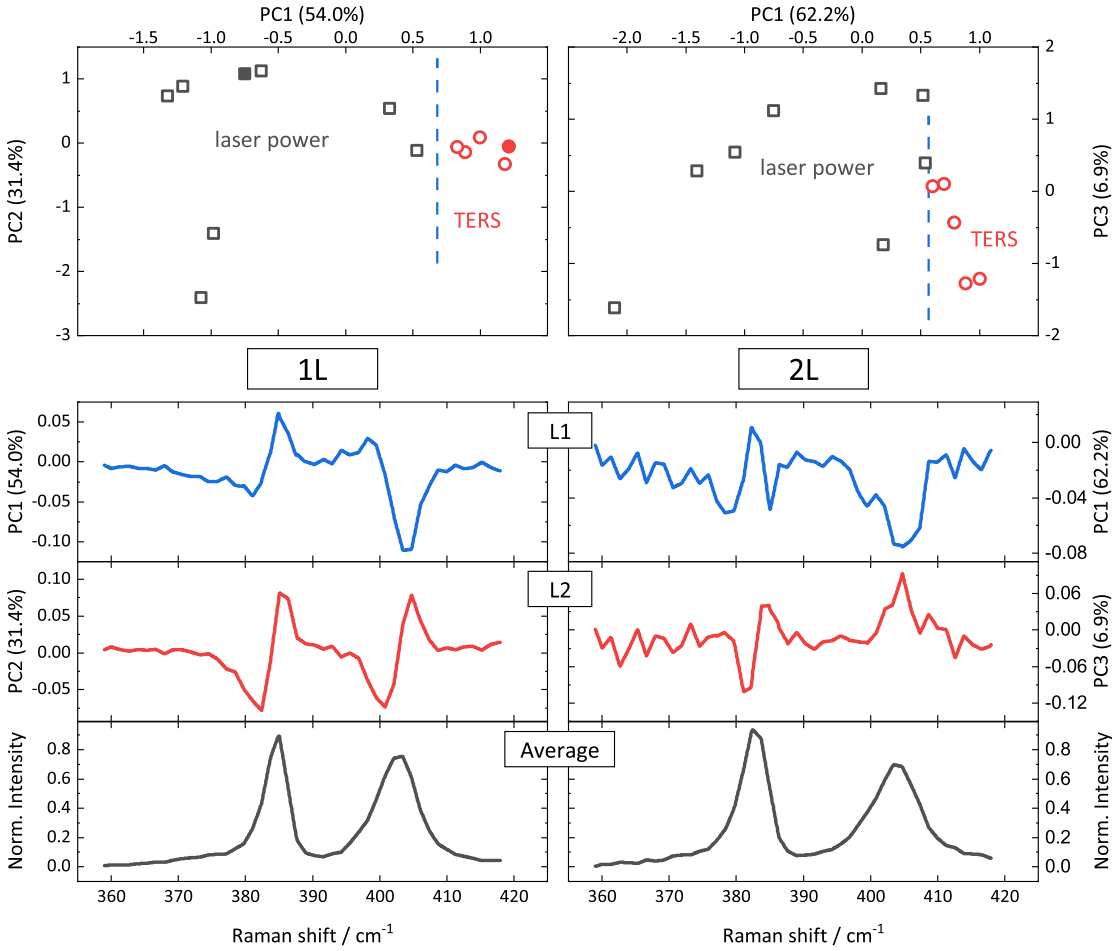

Fig. S6 PCA results of 1L and 2L MoS_2 tip-in and laser power dependent Raman spectra on the left and right, respectively. The upper part shows the PCA score plots. The spectra corresponding to the highlighted (full) symbols are discussed in Fig. S7, in terms of scores and loadings. In both cases the tip-enhanced data are clearly separated from the data of the laser power dependent measurements. The corresponding PC loadings and the average spectra are given in the lower part.

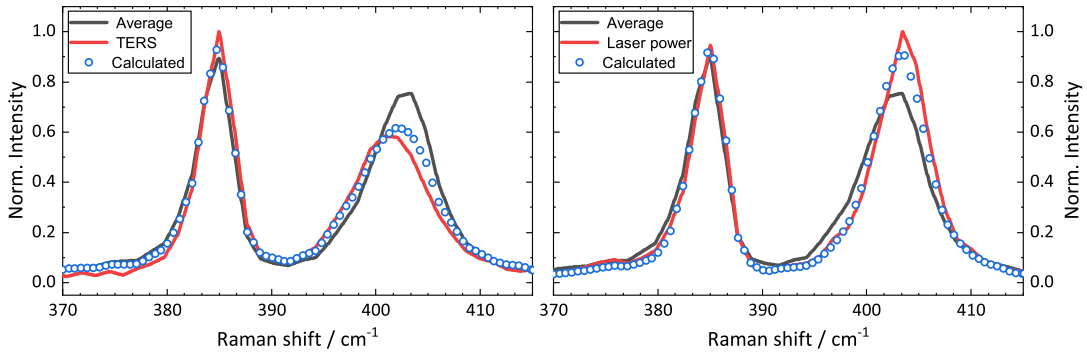

Fig. S7 Display of the average spectrum (black line), the experimental spectrum (red line) and the corresponding recalculated spectrum (blue dots) using Eq. 1, up to i=3. For both exemplary experimental spectra, TERS (left) and laser power dependent (right), the predictions from the PCA results in Fig. S6 could be confirmed.